Stress deprivation of tendon explants or Tpm3.1 inhibition in tendon cells reduces F-actin to promote a tendinosis-like phenotype

Kameron L. Inguito[a], Mandy M. Schofield[a], Arya D. Faghri[a], Ellen T. Bloom[b], Marissa Heino[a,b], Valerie C. West[b], Karl Matthew M. Ebron[c], Dawn M. Elliott[b], and Justin Parreno[a,b,*]
[a]Departments of Biological Sciences, [b]Biomedical Engineering, and [c]Kinesiology and Applied Physiology, University of Delaware, Newark, DE 19716

ABSTRACT **Actin is a central mediator between mechanical force and cellular phenotype. In tendons, it is speculated that mechanical stress deprivation regulates gene expression by reducing filamentous (F)-actin. However, the mechanisms regulating tenocyte F-actin remain unclear. Tropomyosins (Tpms) are master regulators of F-actin. There are more than 40 Tpm isoforms, each having the unique capability to stabilize F-actin subpopulations. We investigated F-actin polymerization in stress-deprived tendons and tested the hypothesis that stress fiber–associated Tpm(s) stabilize F-actin to regulate cellular phenotype. Stress deprivation of mouse tail tendon down-regulated tenogenic and up-regulated protease (matrix metalloproteinase-3) mRNA levels. Concomitant with mRNA modulation were increases in G/F-actin, confirming reduced F-actin by tendon stress deprivation. To investigate the molecular regulation of F-actin, we identified that tail, Achilles, and plantaris tendons express three isoforms in common: Tpm1.6, 3.1, and 4.2. Tpm3.1 associates with F-actin in native and primary tenocytes. Tpm3.1 inhibition reduces F-actin, leading to decreases in tenogenic expression, increases in chondrogenic expression, and enhancement of protease expression in mouse and human tenocytes. These expression changes by Tpm3.1 inhibition are consistent with tendinosis progression. A further understanding of F-actin regulation in musculoskeletal cells could lead to new therapeutic interventions to prevent alterations in cellular phenotype during disease progression.**

Monitoring Editor
Alex Dunn
Stanford University

Received: Feb 28, 2022
Revised: Aug 29, 2022
Accepted: Sep 12, 2022

INTRODUCTION

The dysregulation of filamentous (F)-actin is associated with a wide range of pathologies in load-bearing mechanical tissues (Garbe *et al.*, 2012; Gardiner *et al.*, 2015; Lavagnino *et al.*, 2015a; Tsolis *et al.*, 2015; Neugebauer *et al.*, 2018; Blangy *et al.*, 2020; Li *et al.*, 2020a,b; Hatakeyama *et al.*, 2021; Lee *et al.*, 2021). While the complete interactions between mechanical forces, F-actin, and pathology are not fully clear, the actin cytoskeleton may be a key mediator between mechanical force and cellular phenotype (Ralphs *et al.*, 2002; Jarvinen *et al.*, 2003; Lavagnino and Arnoczky, 2005; Chen *et al.*, 2015; Hatakeyama *et al.*, 2021; Lee *et al.*, 2021). Tendon is an ideal tissue model to examine the mechanical regulation of cellular phenotype (Thornton *et al.*, 2010). Mechanical loading of tendon is essential to maintain tissue homeostasis, and tissue overloading is a cause of tendinosis (Kjaer *et al.*, 2009; Zhang and Wang, 2013; Huisman *et al.*, 2014; Wang *et al.*, 2015; Mubyana and Corr, 2018; Fleischhacker *et al.*, 2020; Sawadkar *et al.*, 2020). While it may be speculated that tendon overload leads to mechanical overstimulation of residing tendon cells, leading to alterations in cell phenotype (i.e., matrix metalloproteinase [Mmp] production) (Lo *et al.*, 2004a; Thornton *et al.*, 2010), an alternative hypothesis is that overload leads to a paradoxical mechanical understimulation or stress deprivation of tendon cells (Arnoczky *et al.*, 2007a; Lavagnino *et al.*, 2015b). The hypothesized disruption of cell–matrix interactions during overload results in the failure of loads to be transmitted to cells.

This article was published online ahead of print in MBoC in Press (http://www.molbiolcell.org/cgi/doi/10.1091/mbc.E22-02-0067 on September 21, 2022).

*Address correspondence to: Justin Parreno (jparreno@udel.edu).

Abbreviations used: Acan, Aggrecan; {alpha}sma, alpha smooth muscle actin; Col1, Type I collagen; F-actin, filamentous actin; G-actin, globular actin; Mmp3, Matrix Metalloproteinase-3; Mmp13, Matrix Metalloproteinase-13; Scx, Scleraxis; Sox9, SRY-Box Transcription Factor 9; Tnc, Tenascin-C; Tpm, Tropomyosin.

In support of this hypothesis, overloading of rat tail tendon resulted in cell–matrix disruptions as demonstrated using transmission electron microscopy by an increase in spacing between matrix and cells (Ros *et al.*, 2019).

Mechanical stress deprivation of explant tendon tissue has been widely used to investigate the connection between cellular understimulation and tissue degeneration. Unloading or stress-depriving tendons by culturing explants in the absence of mechanical load recapitulates several aspects of tendinosis. Stress deprivation alters the tendon cell phenotype, causing a reduction in tendon molecule (such as collagen-1; Col1) expression and enhancement of matrix degradation molecule (such as Mmps) expression as compared with tendons freshly isolated from a mechanically stressed in vivo environment (Lo *et al.*, 2004b; Lavagnino *et al.*, 2006, 2008; Arnoczky *et al.*, 2007b, 2008; Gardner *et al.*, 2008; Wunderli *et al.*, 2018; Jafari *et al.*, 2019; Stauber *et al.*, 2020; Egerbacher *et al.*, 2022). However, stretching tendons while in culture prevents these tendinosis-like changes. The protective effects of stretch are abrogated if stretched tendons are cultured in the presence of cytochalasin D, which caps barbed ends of actin to prevent F-actin polymerization (Arnoczky *et al.*, 2004; Lavagnino and Arnoczky, 2005). These findings have led to the speculation that stress deprivation regulates tendon cell phenotype via a reduction of F-actin where an increase in monomeric, globular (G)-actin has been shown in other cell types to regulate gene expression (Parreno *et al.*, 2014, 2017, 2020; Delve *et al.*, 2020). However, there are limited data to support that stress deprivation reduces F-actin. In the present study, we ask, is F-actin reduced during tendon stress deprivation? To answer this, we performed whole-mount confocal imaging followed by image quantification to compare freshly isolated stress-deprived tendons stained for F- and G-actin. We confirm that the acquisition of tendinosis-like molecular expression by stress deprivation correlates with a reduction in F-actin.

Our finding of reduced F-actin prompted us to examine the molecular regulation of F-actin in tendon cells. We focused on the regulation of F-actin networks by tropomyosin (Tpm), the master regulator of F-actin that binds along and stabilizes F-actin (Gunning *et al.*, 2015). The regulation of tenocyte F-actin by Tpms is largely unknown. In native and in vitro (primary cultured) tendon cells, F-actin organizes into stress fibers (Ralphs *et al.*, 2002) containing α-smooth muscle actin (αsma), a highly contractile form of actin (Khan *et al.*, 1999; Premdas *et al.*, 2001; Ralphs *et al.*, 2002; Chen *et al.*, 2015). Tpm associates with F-actin stress fibers in tendon cells (Ralphs *et al.*, 2002). However, the particular Tpm(s) expressed within tendon cells are not clear. More than 40 isoforms of mammalian tropomyosin exist, and each isoform has the unique capability to stabilize specific F-actin subpopulations. Thus, the particular Tpm(s) expressed within a cell defines overall F-actin organization.

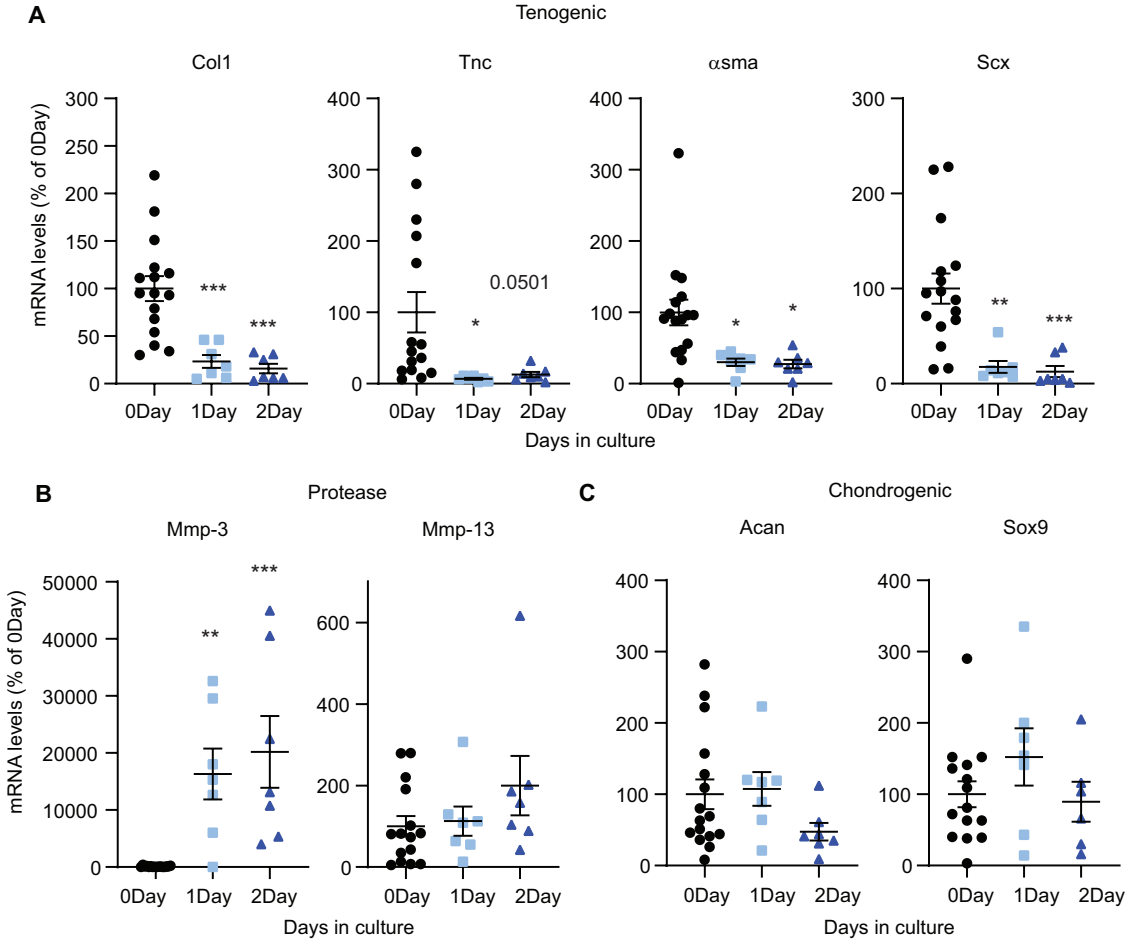

FIGURE 1: Stress deprivation recapitulates aspects of tendinosis gene expression. Relative real-time PCR of tendons in 1 or 2 d stress deprivation culture as compared with freshly isolated (0 d) tendons demonstrating (A) a reduction in tenogenic marker mRNA levels, (B) an increase in MMP-3 mRNA levels, and (C) no change in chondrogenic mRNA levels. Specific mRNA levels were normalized to Gapdh, and normalized values are expressed as a percent of freshly isolated (0 d) controls. Mean ± SEM is indicated on dot plots. *, $p < 0.05$; **, $p < 0.01$; ***, $p < 0.001$.

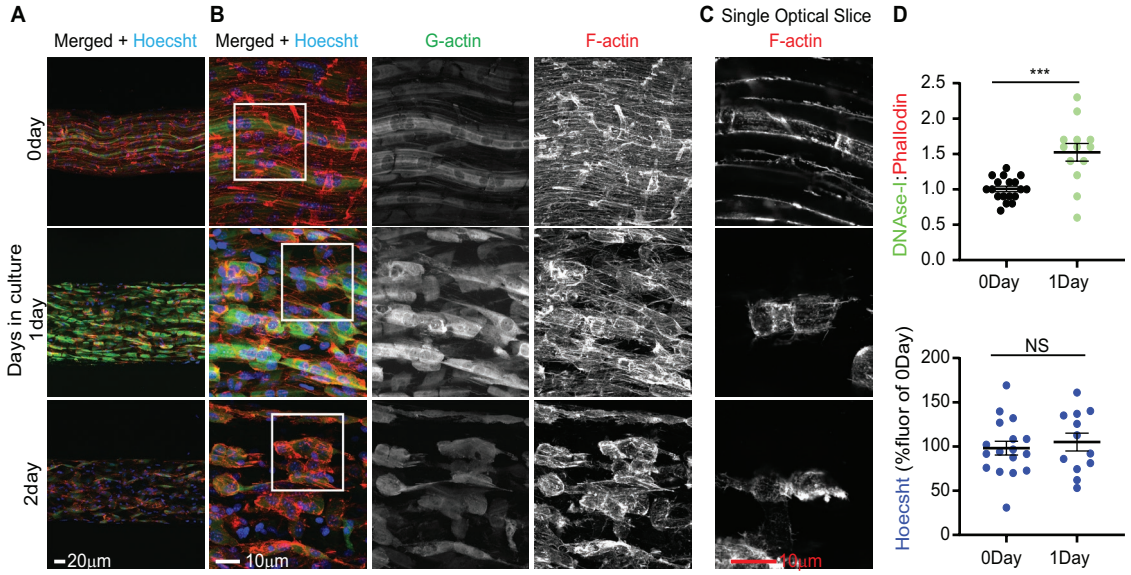

FIGURE 2: Stress deprivation alters tendon cell morphology and destabilizes F-actin. (A, B) Maximum-intensity projection images of tendons demonstrating an increase in G/F-actin staining after 1 d of culture taken with either a 20× (panel A) or a 63× (panel B) objective. In panel B, grayscale images represent individual channels for G- and F-actin. (C) Single optical slice of boxed region in panel B demonstrates that cell morphology and F-actin are altered by stress deprivation. (D) Dot plots of DNaseI:phalloidin to demonstrate an increase in G/F-actin. Mean ± SEM is indicated on dot plots. Average DNaseI:phallodin for controls was set to 1.0, and 1 d stress-deprived values were scaled accordingly. Nuclei staining intensity using Hoechst was calculated to demonstrate that there were no significant differences in staining between control and stress-deprived tendons. Average fluorescence intensities for controls were set to 100%, and stress-deprived tendon intensities are expressed as relative percentage to controls. ***, $p < 0.001$.

In this study, we aimed to determine which Tpm isoforms are expressed by tendon cells. Because tenocyte F-actin networks arrange into stress fibers, we focused on elucidating the function of stress fiber–associated Tpm isoforms. Previous studies using osteosarcoma (U2OS) cells have indicated that at least six Tpms (1.6, 1.7, 2.1, 3.1, 3.2, and 4.2) are associated with stress fibers (Tojkander *et al.*, 2011; Gateva *et al.*, 2017). In lens epithelial cells, we demonstrated that inhibition of just one Tpm isoform (Tpm3.1) prevents stress fiber formation resulting in downstream gene modulation (Parreno *et al.*, 2020). Therefore, in this study we tested the hypothesis that stress fiber–associated Tpm(s) stabilize tenocyte F-actin and regulate cellular phenotype by modulating mRNA levels.

It is essential to unravel how cellular phenotype is determined by the F-actin network's response to mechanical forces and to elucidate the molecules that determine F-actin networks. Establishing the mechanisms involved in regulating cellular phenotype by F-actin in pathological processes, such as tendon overload, could lead to new therapeutic opportunities against disease.

RESULTS

Tendon stress deprivation results in tendinosis-like gene changes

Tendinosis progression is characterized by a decrease in tenogenic gene expression, an up-regulation of degradative genes, and ectopic expression of cartilage genes (Lo *et al.*, 2004b; Lavagnino *et al.*, 2006; Arnoczky *et al.*, 2007b, 2008; Gardner *et al.*, 2008; Lavagnino *et al.*, 2008; Yuan *et al.*, 2016; Bell *et al.*, 2018; Wunderli *et al.*, 2018; Jafari *et al.*, 2019; Stauber *et al.*, 2020; Chatterjee *et al.*, 2022; Egerbacher *et al.*, 2022). Tendon stress deprivation, ex vivo, has been shown to recapitulate several aspects of tendinosis gene modulation. We evaluated the effect of stress deprivation on tail tenocyte gene expression by culturing mouse tail tendon fascicles in the absence of stretch for up to 2 d.

Stress deprivation decreases tenogenic mRNA levels (Figure 1A). We observe a decrease in Col1, the predominant collagen expressed in tendons (Sharma and Maffulli, 2006; Sbardella *et al.*, 2014; Chatterjee *et al.*, 2022), and a decrease in tenascin C (Tnc), a mechanosensitive matricellular glycoprotein present in tendon matrix that assists in the structural arrangement of collagen fibers as well as providing for tissue elasticity (Jarvinen *et al.*, 2003; Nemoto *et al.*, 2013; Sbardella *et al.*, 2014). In addition, we observe a reduction in Scx, a transcription factor that drives tenogenic expression, such as the expression of collagen-1 (Lejard *et al.*, 2007; Bagchi and Czubryt, 2012). Finally, we detect a decrease in α-smooth muscle actin (αsma), an actin isoform present in tendon cells, which is thought to be necessary for recovery of tendon cells following stretch (Chatterjee *et al.*, 2022).

Stress deprivation enhances the expression of specific degradative molecules (Figure 1B). Mmp-3 and Mmp-13 have been implicated in tendinosis and are up-regulated during stress deprivation (Lo *et al.*, 2004a; Lavagnino and Arnoczky, 2005; Lavagnino *et al.*, 2006; Sharma and Maffulli, 2006; Arnoczky *et al.*, 2008; Parreno *et al.*, 2008). We determine that Mmp-3 is up-regulated 163.1-fold at 1 d and 201.9-fold at 2 d (Figure 1B). Unlike in previous studies (Lavagnino *et al.*, 2006), we did not observe an increase in Mmp-13 mRNA levels at 1 or 2 d postculture.

An increase in chondrogenic expression is a feature of tendinosis (Yuan *et al.*, 2016) but is not recapitulated by tendon stress deprivation. We observed no significant effect on chondrogenic (Acan or Sox9; Figure 1C) mRNA levels up to 2 d of stress deprivation (Figure 1C). Thus, in vitro stress deprivation of tail tendons recapitulates certain, but not all, aspects of tendinosis.

Stress deprivation promotes cell rounding and destabilizes tenocyte F-actin

We found that tendon stress deprivation alters tenocyte morphology and F-actin depolymerization (Lavagnino and Arnoczky, 2005;

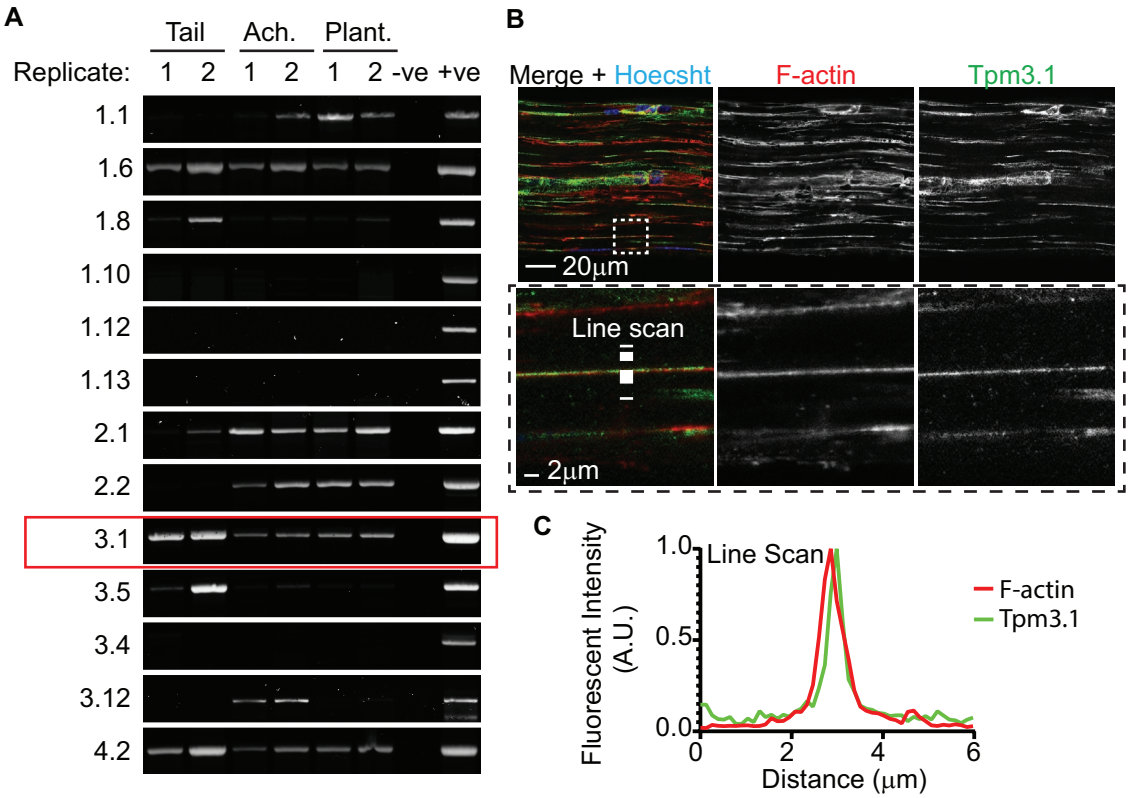

FIGURE 3: Tpm isoform expression is dependent on tendon type, but all three types examined express Tpm3.1. (A) Semiquantitative PCR for Tpms in native tail, Achilles (Ach.), and plantaris (Plant.) tendons. (B, top panels) Whole-mount immunostaining shows distribution of Tpm3.1 throughout tail tendon. (B, bottom panels) High-magnification images of dashed area show association of Tpm3.1 along with F-actin. (C) Line scan analysis showing colocalization of Tpm3.1 with F-actin.

Lavagnino *et al.*, 2015a; Chen *et al.*, 2015). To determine whether F-actin depolymerization occurs in native tendons, we performed whole-mount imaging of tendons stained with DNase-I and phalloidin to visualize G- and F-actin, respectively. Tendon cells from freshly isolated tendons are elongated and have parallel F-actin networks regarded as stress fibers throughout the tissue (Ralphs *et al.*, 2002) (Figure 2, A and B). Stress deprivation results in rounded tendon cells. We also observe a reduction of F-actin in stress fibers. Fluorescent image quantification reveals that stress deprivation elevates G/F-actin staining after 1 d compared with freshly isolated controls (Figure 2C). By 2 d of culture, despite differences in F-actin network organization, G/F-actin status is similar to that in controls (unpublished data). Our findings confirm that stress deprivation destabilizes F-actin.

These results support the idea that a reduction of F-actin regulates tendinosis gene changes. Tpms are known master regulators of F-actin; therefore we next focused on characterizing the role of Tpms in tendon cells.

Tpm expression in native tendon cells

Tpm isoforms have the unique ability to stabilize specific F-actin networks (Bryce *et al.*, 2003; Schevzov *et al.*, 2011; Gunning *et al.*, 2015; Gateva *et al.*, 2017). Therefore, we first sought to determine which Tpm isoforms are expressed by tendon cells. Tpm expression is variable and dependent on tendon type. To determine specific Tpm isoform expression within various tendon types (tail, Achilles, and plantaris), we used semiquantitative real-time-PCR (RT-PCR) analysis, followed by Sanger sequencing of cDNA products. Collectively, in total, we found that tendons express nine Tpm isoforms: Tpm1.1, 1.6, 1.8, 2.1, 2.2, 3.1, 3.5, 3.12, and 4.2. However, the specific Tpms expressed are dependent on tendon type. Only three of the nine Tpm isoforms are consistently expressed in all three tendon types tested: Tpm1.6, 3.1, and 4.2.

In this study we chose to focus on the regulation of F-actin networks by Tpm3.1, as we previously have shown it to regulate stress fibers in lens epithelial cells (Parreno *et al.*, 2020). Furthermore, there are established inhibitors toward Tpm3.1, including TR100 (Bonello *et al.*, 2016; Kee *et al.*, 2018). To confirm Tpm3.1 protein expression and association with F-actin, we performed whole-mount immunostaining of the tail fascicle using antibody 2G10.2, which recognizes the 9D exon of Tpm3.1. Our findings indicate Tpm3.1 expression within native tail tendon cells. Furthermore, line scan analysis shows overlap in signal between Tpm3.1 and phalloidin staining, suggesting that Tpm3.1 associates with native F-actin stress fibers (Figure 3C).

Inhibition of Tpm3.1 with TR100 alters tenocyte morphology

To determine Tpm3.1 function in tendon cells, we used primary tendon cells isolated from tail tendon fascicles. Primary tendon cells retain stress fiber organization of F-actin (Ralphs *et al.*, 2002). Furthermore, cultured cells devoid of matrix are more amenable to biochemical assays (i.e., Triton-based cellular fractionation) than native tissues.

We exposed cultured tendon cells to a small molecule inhibitor of Tpm3.1, TR100 (Stehn *et al.*, 2013; Bonello *et al.*, 2016;

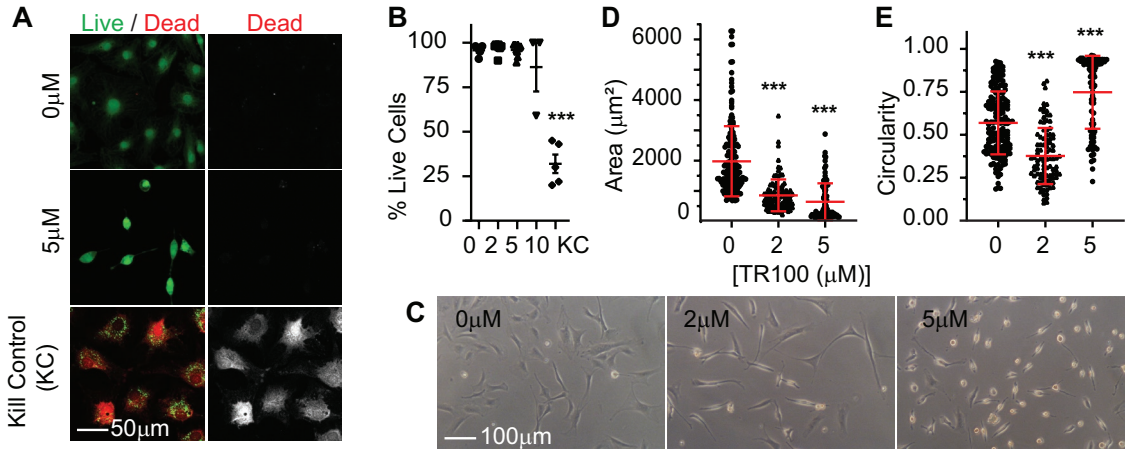

FIGURE 4: Exposure of cells to TR100 alters tenocyte shape and size. (A) Tendon cells are viable following 1 d treatments of TR100 up to 5 μM as seen by positive staining for live cell stain (calcein AM; green) and negative staining for dead cell stain (propidium iodide; red). Cells fixed in 70% EtOH for 15 min served as dead controls (kill control; KC). (B) Dot plot showing the percentage of cells that are alive following treatments as measured by propidium iodide exclusion counts. Mean ± SEM is indicated on dot plots. (C) Light microscopy images of cells treated with TR100 and corresponding dot plots demonstrating changes to tenocyte (D) cell area and (E) circularity. (D, E) Mean ± SD is indicated on dot plots. ***, $p < 0.001$.

Janco *et al.*, 2019). TR100 nullifies the ability of Tpm3.1 to protect actin filaments from depolymerization when present during copolymerization of actin with Tpm3.1. It is suspected that TR100 incorporates into the head-to-tail overlap junction of Tpm3.1 and with prolonged exposure, breakdown of Tpm3.1 containing actin filaments may occur. Live/dead staining (Figure 4A) and propidium iodide exclusion assay (Figure 4B) demonstrate that treating tendon cells with ≤5 μM TR100 retains cell viability. To determine the effect of Tpm3.1 inhibition on cell morphology, we performed light microscopy followed by image quantification (Figure 4C). Both 2 and 5 μM TR100 decrease overall cell area (Figure 4D). Interestingly, while 2 μM TR100 induces tenocyte elongation (decrease in circularity), exposure to 5 μM TR100 causes cell rounding (increase in circularity).

Tpm3.1 stabilizes tenocyte F-actin

We sought to determine whether Tpm3.1 regulates tenocyte F-actin. Confocal microscopy demonstrates that stress fibers are present in control cells as well as in cells treated with 2 μM TR100 (Figure 5, A and B). Treatment with 5 μM TR100 represses F-actin stress fibers and results in cortically arranged Tpm3.1 and F-actin in a subpopulation of cells. This cortical F-actin network arrangement is completely absent in control cells and in cells treated with 2 μM TR100, whereas it is present in 58.2 ± 8.1% (mean ± SE) of cells treated with 5 μM TR100.

Next, we evaluated G/F-actin proportion in TR100-treated cells using Triton fractionation followed by WES-capillary electrophoresis (Figure 5, C–E). Treatment with TR100 increases the amount of actin present in soluble portions indicative of elevated G-actin (Figure 5, D and E). On average, there is a significant increase in the proportion of G/F-actin by treatment with 5 μM TR100. While 2 μM TR100 appears to result in a slight increase in the proportion of G/F-actin, this was not statistically significant ($p = 0.42$).

TR100 treatment results in tendinosis-like gene changes

Our findings (Figure 5) reveal that Tpm3.1 regulates F-actin in tendon cells. The findings that the reduction of F-actin regulates tendinosis-like gene changes (Figure 1) led us to next testing the hypothesis that Tpm3.1 inhibition will induce down-regulation of tenogenic genes and up-regulation of protease and chondrogenic expression.

We determined that reduction of F-actin by TR100 treatment decreases tenogenic mRNA levels. This was apparent at both 2 and 5 μM treatments. With 5 μM treatment of TR100, there are 21.2-, 1.4-, 29.2-, and 2.5-fold decreases in Col1, Tnc, αsma, and Scx, respectively (Figure 6). Treatment with 5 μM TR100 also up-regulates protease expression, resulting in 18.1- and 374.3-fold increases in Mmp-3 and Mmp-13, respectively. Finally, exposure of cells to 5 μM TR100 up-regulates chondrogenic mRNA levels, resulting in 3.4- and 9.2-fold increases in Acan and Sox9, respectively. We found that only the 5 μM treatment, but not the 2 μM treatment, up-regulates protease and chondrogenic levels.

Next, we sought to determine whether TR100 induced gene changes in mouse tenocytes similarly occur in human tenocytes. We examined select tenogenic, protease, and chondrogenic genes via real-time RT-PCR and found that TR100 decreases Col1, as well as increasing Mmp13 and Sox9 mRNA levels in human tenocytes (Figure 7).

Finally, we examined modulation of mouse tenocyte protein expression by 5 μM TR100 treatment on select molecules using immunostaining followed by quantitative image analysis (SCX) or via capillary electrophoresis (αSMA and MMP-3). TR100 decreases the total nuclear fluorescent staining for SCX in tendon cells (Figure 8, A and B) as well as the proportion of nuclear/cytosplasmic SCX (Figure 8, A and C). Additionally, TR100 decreases αSMA protein levels by 2.0-fold (Figure 8, D–F). Finally, TR100 increases MMP-3 protein levels by 14.3-fold (Figure 8, D–F). Modulation of SCX, aSMA, and MMP-3 is consistent between mRNA and protein levels.

DISCUSSION

This study provides novel insight into the regulation of the pathological cellular phenotype by F-actin. We determined that tendinosis-like gene changes caused by stress deprivation coincide with a reduction in F-actin. This result led us to investigate the molecular regulation of F-actin by Tpms, which are known to stabilize F-actin. We revealed that tendons express several Tpm isoforms, including Tpm3.1, a stress fiber–associated Tpm (Tojkander *et al.*, 2011; Gateva *et al.*, 2017; Parreno *et al.*, 2020). We found that Tpm3.1 associates with F-actin networks in tendon cells and regulates the

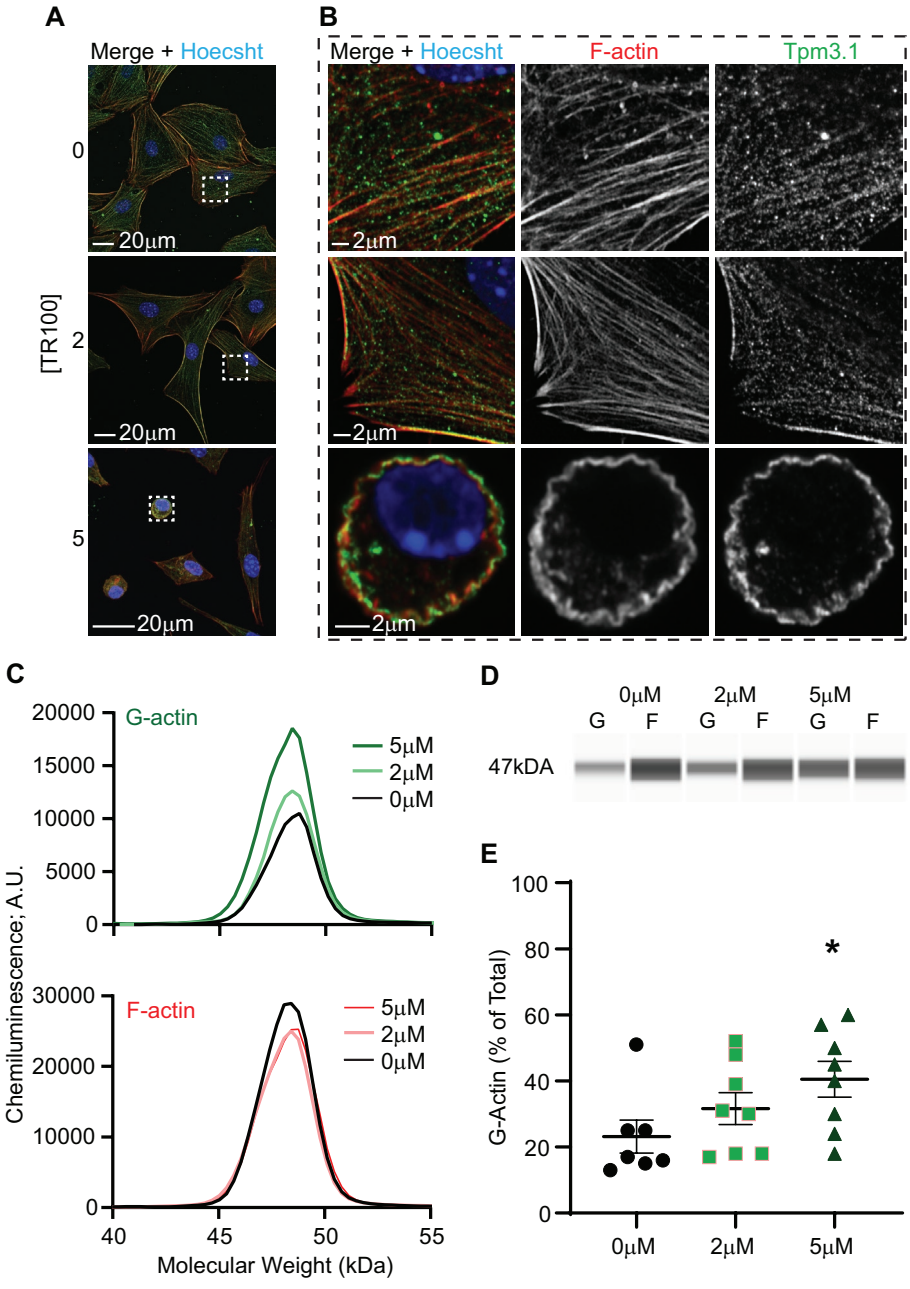

FIGURE 5: Tpm3.1 inhibition reduces F-actin stress fibers and increases G/F-actin. (A) Maximum-intensity projection images of tendon cells following 1 d treatment of TR100, demonstrating that TR100 reduces F-actin bundles organized into stress fibers. Images taken with a 20× objective. (B) Single optical slice images of boxed regions, demonstrating reduction of F-actin bundles in stress fibers and the acquisition of cortical organization of Tpm3.1 and F-actin (5 μM TR100). Images taken with a 63× objective. (C) Capillary Western blot (WES) immunoassay electropherogram of Triton-fractionated samples. The Triton-soluble fraction is indicative of G-actin (top panel), and the Triton-insoluble fraction is indicative of F-actin. (D) Virtual gel showing actin bands at approximately 47 kDa. (E) Corresponding dot plots showing that the proportion of G-actin within cells increases by treatment with 5 μM TR100. Mean ± SEM is indicated on dot plots. *, $p < 0.05$.

tenocyte cellular phenotype. Tpm3.1 inhibition reduces F-actin stress fibers, causing a robust tendinosis-like gene response.

Our data support the speculation that stress deprivation regulates cellular phenotype by a reduction of F-actin (Arnoczky *et al.*, 2004). Previously it was shown that tendon stress deprivation increases Mmp mRNA levels (Arnoczky *et al.*, 2004; Wunderli *et al.*, 2018). It was also demonstrated that stretching in vitro–cultured tendons can repress Mmp up-regulation (Arnoczky *et al.*, 2004; Wunderli *et al.*, 2018). Mechanical stretch appears to regulate Mmp expression via actin-based mechanisms as treating stretched tendons with cytochalasin D, which caps F-actin. preventing actin polymerization, abrogates the protective effects of stretch (Arnoczky *et al.*, 2004). This led to the speculation that stress deprivation regulates Mmp expression via actin depolymerization. However, evidence for reduced F-actin in stress deprivation was still required. In the current study, we provide empirical evidence that stress deprivation destabilizes F-actin, as demonstrated by an increase in G/F-actin staining (Figure 2). We show that this increase in G/F-actin coincides with an increase in protease expression (Mmp-3) (Figure 1). This finding is consistent with our previous findings in bone cells, where stress deprivation of osteoblast-like MG-63 cells in collagen gels enhances Mmp-3 gene expression (Parreno *et al.*, 2008). Unlike other previous studies, Mmp-13 was not found to be up-regulated, although there was a trend toward an increase in Mmp-13 expression by day 2 ($p = 0.17$). Previous studies examined Mmp expression at later time points (i.e., up to 10 d of stress deprivation) (Jafari *et al.*, 2019), which could explain the discrepancy in the Mmp-13 response. Note that we did not examine Mmp-1 expression here, as it is not expressed in mice. Nevertheless, our findings indicate that a reduction of F-actin corresponds to an increase in Mmp-3, a protease that plays a role in tendinosis (Raleigh *et al.*, 2009). The reduction of F-actin appears to be an important regulator of Mmps during disease processes like tendinosis.

We attribute the alterations in mRNA levels and F-actin seen in the current study to stress deprivation of tendons in culture. However, unlike the ex vivo culture condition where tenocytes are exposed to higher levels of oxygen and serum, healthy tenocytes in vivo exist in an environment that is minimally vascularized and oxygenated. Therefore, it is arguable that other culture factors may influence the tenocyte cellular response (Wunderli *et al.*, 2018, 2020). In a previous study, using a bespoke loading device to mechanically stimulate mouse tendons, it was shown that the application of an intermittent uniaxial cyclic stretch on cultured mouse tail tendons enhanced Col1 and Scx as well as reducing Mmp-3 mRNA (Wunderli *et al.*, 2018). The stretched mRNA levels approximated freshly isolated tendon mRNA levels. Furthermore, F-actin organization was markedly different between stretched and stress deprived, under

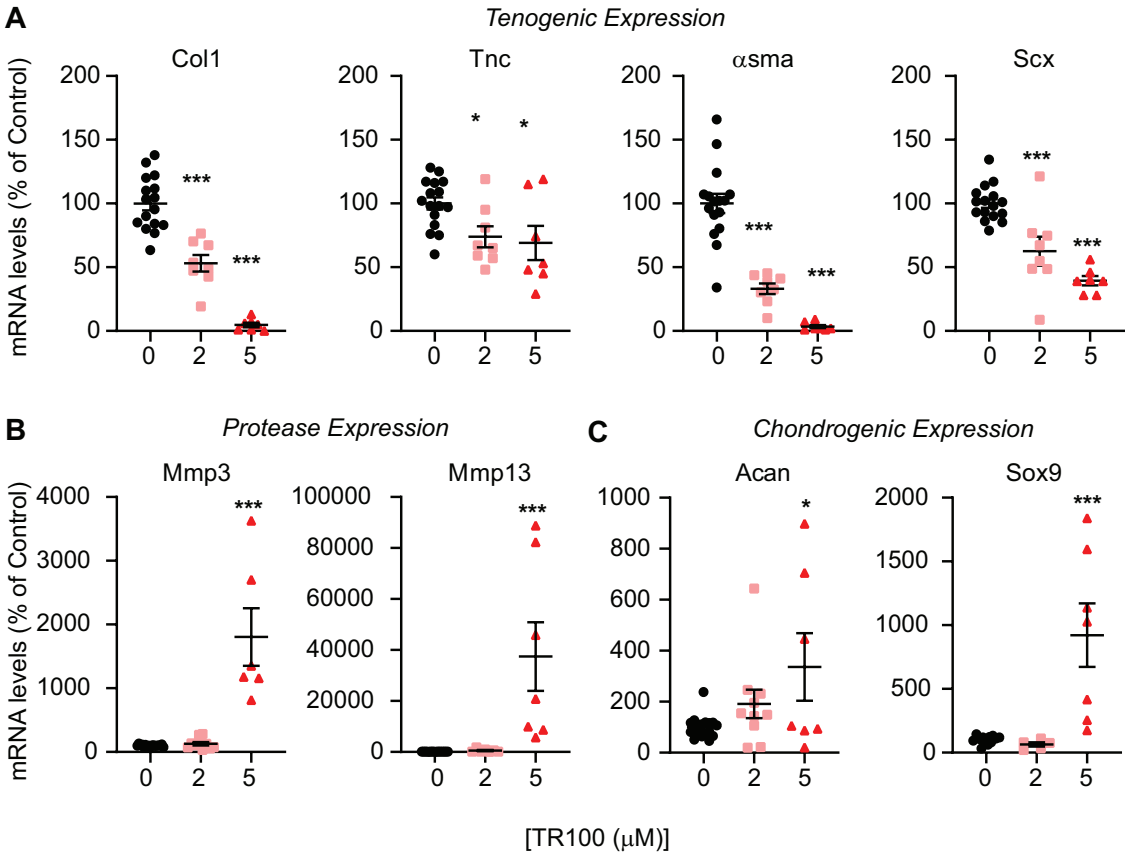

FIGURE 6: Reduction of F-actin by inhibition of Tpm3.1 results in tendinosis-like gene modulation in mouse tenocytes. Relative real-time PCR of tendon cells treated with 0, 2, or 5 μM TR100 for 1 d demonstrating (A) a reduction in tenocyte marker mRNA levels and (B) an increase in protease mRNA levels and (C) chondrogenic mRNA levels. Specific mRNA levels were normalized to Gapdh, and normalized values are expressed as a percent of nontreated (0 μM) controls. Mean ± SEM is indicated on dot plots. *, $p < 0.05$; ***, $p < 0.001$.

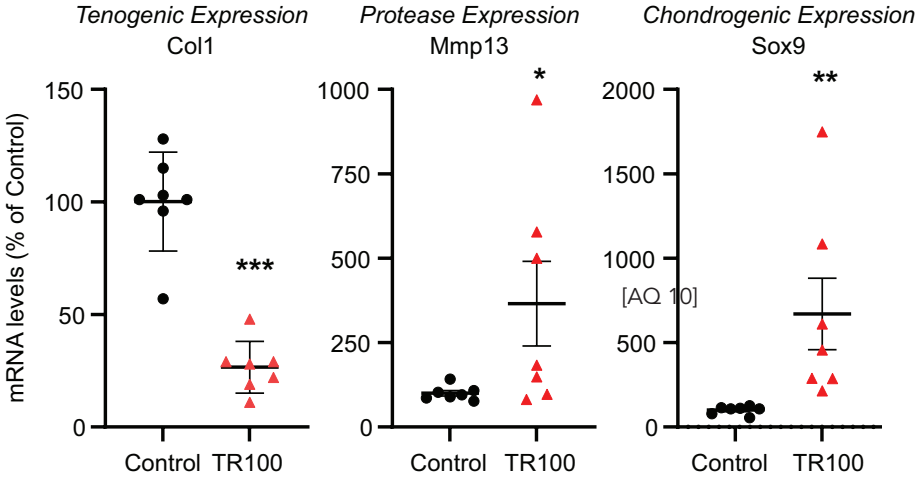

FIGURE 7: Reduction of F-actin by inhibition of Tpm3.1 results in tendinosis-like gene modulation for select genes in human tenocytes. Relative real-time PCR of human tendon cells treated with 4 mM TR100 for 1 d demonstrating a reduction in tenocyte marker (Col1) mRNA levels and an increase in protease (Mmp13) and chondrogenic (Sox9) mRNA levels. Specific mRNA levels were normalized to 18S, and normalized values are expressed as a percent of nontreated controls. Mean ± SEM is indicated on dot plots. *, $p < 0.05$; **, $p < 0.01$, ***, $p < 0.001$.

otherwise identical culture conditions. Therefore, stress deprivation appears to be a predominant factor regulating cellular response in the ex vivo stress–deprived tendon explant culture system.

We sought to determine the regulation of F-actin by Tpms and found that tendon cells express several Tpm isoforms, including several known stress fiber-associated Tpms (Figure 3). Previously, Ralphs *et al.* (2002) indicated the presence of Tpm in tendon cells using Western blotting and immunofluorescence. However, Tpm antibodies are developed using peptides that correspond to specific exons that are highly conserved between various Tpms (Schevzov *et al.*, 2011). Thus, antibodies are specific to exons and not to particular isoforms. The particular (TM311) antibody used by Ralphs *et al.* (2002) recognizes an epitope on exon 1A of Tpm1 and 2 (Schevzov *et al.*, 2011). Therefore, it remained unclear which exact Tpm isoform was expressed in tendons. In our present study, we determined that

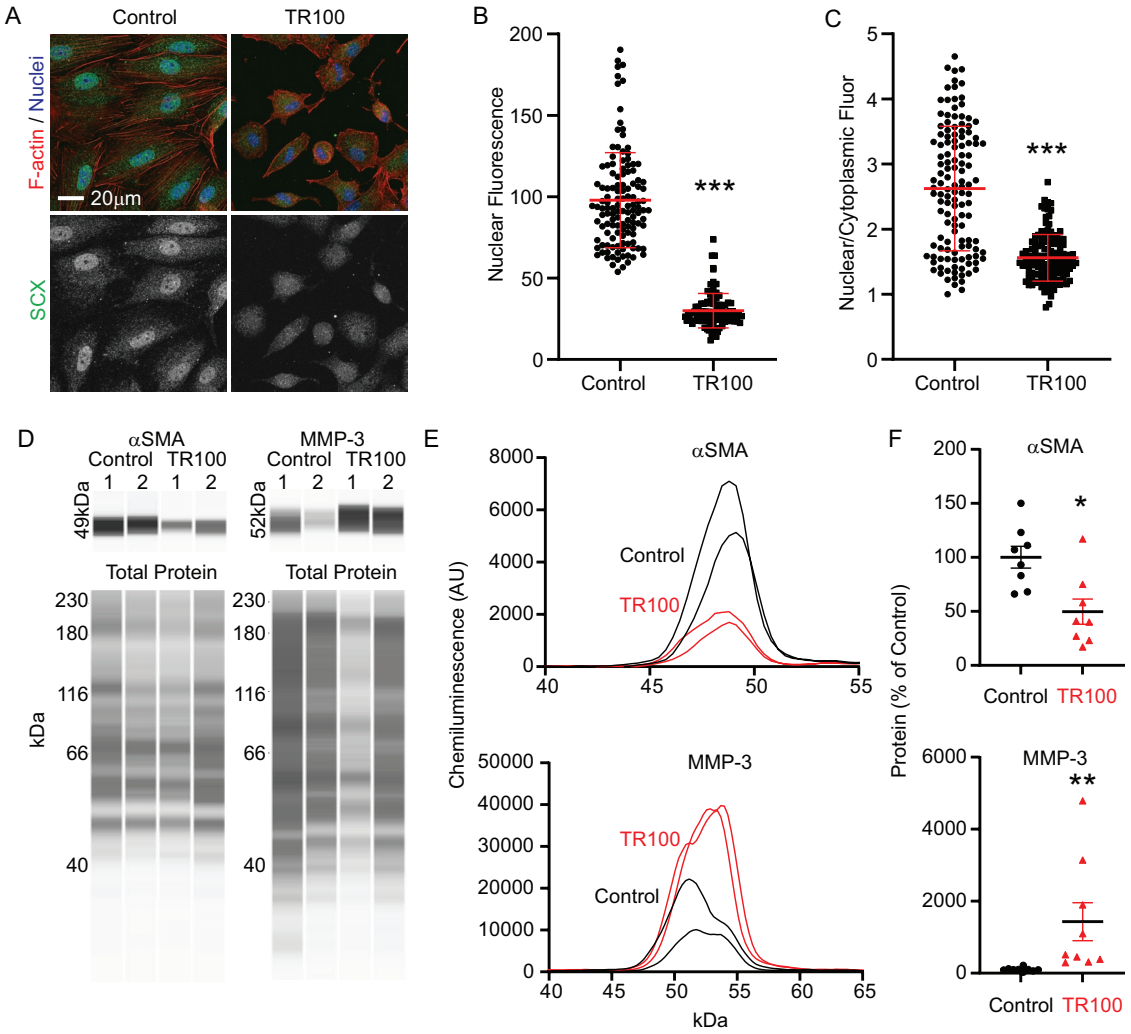

FIGURE 8: Modulation of select protein levels by TR100 (5 μM) treatment after 2 d of treatment. (A) Representative fluorescence confocal microscopy images for SCX. (B) Total nuclear fluorescence for SCX in individual cells, expressed as a percentage of mean nuclear fluorescence of control cells. (C) Calculated nuclear/cytoplasmic ratio of SCX for individual cells. Mean ± SD is indicated on dot plots in B and C. Representative WES electrophoresis data showing (D) pseudo-Western blots with corresponding (E) electropherograms for αSMA and MMP-3. (F) αSMA and MMP-3 protein after normalization to total protein. Protein levels are expressed as a percentage of untreated controls. Mean ± SEM is indicated on dot plots. *, $p < 0.05$; **, $p < 0.01$; ***, $p < 0.001$.

tendon cells can express 9 Tpms: Tpm1.1, 1.6, 1.8, 2.1, 2.2, 3.1, 3.5, 3.12, and 4.2. On the basis of our data, we believe that Ralphs *et al.* (2002) could have been probing for Tpms 1.1, 1.6, 2.1, 2.2. Tpm2.1 has been identified as a stress-fiber associated Tpm (Gateva *et al.*, 2017). However, it is not present in all tendons, specifically tail tendons. The variation of Tpm isoform expression between tendons from different anatomical regions is surprising and unexpected. We predict that Tpm isoform variation in different tendon types reflects the formation of unique F-actin networks to meet individual varying functional demands of specific tendon types (Lee and Elliott, 2019). Intriguingly, out of the nine Tpm isoforms expressed by tendon, we found that only three isoforms were consistently expressed in all tendons (tail, Achilles, plantaris) examined: Tpm1.6, 3.1, and 4.2. The presence of these three isoforms in multiple tendon types could indicate that these isoforms are critical for general tendon function. Two of these isoforms, Tpm3.1 and 4.2, are known stress fiber–associated Tpms. We chose to focus on Tpm3.1 as we previously showed it to be a crucial regulator of F-actin stress fibers in lens epithelial cells (Parreno *et al.*, 2020). The present study is the first, to our knowledge, to examine Tpm3.1 in tendon cells.

Tpm3.1 associates with F-actin in native tendon cells as well as in vitro–cultured tendon cells to maintain F-actin stress fibers (Figure 3). The association of Tpm3.1 with stress fibers in tendon cells is in agreement with past studies on lens epithelial (Parreno *et al.*, 2020), human osteosarcoma (U2OS) (Tojkander *et al.*, 2011; Gateva *et al.*, 2017; Meiring *et al.*, 2019; Zhao *et al.*, 2020), human neuroblastoma (SK-N-BE(2)) (Pathan-Chhatbar *et al.*, 2018), and neuronal (B35) (Bryce *et al.*, 2003) cells. Tpm3.1 maintains F-actin networks through regulation of other actin-associated molecules. It has been shown to promote the activation of nonmuscle myosin activity (Bryce *et al.*, 2003; Tojkander *et al.*, 2011; Gateva *et al.*, 2017; Pathan-Chhatbar *et al.*, 2018) as well as interfering with the association of severing molecules (i.e., cofilin) onto actin (Bryce *et al.*, 2003). Here, we show that inhibition of Tpm3.1 results in the reduction of F-actin (Figure 5), leading to tendinosis-like molecule modulation in both mouse and human tenocytes (Figures 6–8). The

tendinosis-like gene modulation, however, was dose dependent. In mouse tenocytes we found that tenogenic genes are responsive to 2 μM treatments of TR100, whereas protease and chondrogenic genes are not significantly altered. This suggests that tenogenic genes are more sensitive to perturbations of F-actin. It is possible that multiple signaling mechanisms downstream of actin regulate tenogenic gene expression, amplifying the effects of subtle actin perturbation. Of note, there was a trend toward an increase in G/F-actin by exposure of cells to 2 μM TR100 treatment; however, this was not significant. Biochemical analysis of G/F-actin may be a limitation to detecting subtle differences (<10%) in actin polymerization.

Surprisingly, as compared with stress deprivation of tendons, TR100 treatment of cells had a more substantial effect on the number of genes affected. Stress deprivation of tendons decreased tenogenic expression but unlike TR100 treatment of cells did not enhance chondrogenic genes (Khan *et al.*, 1999). Additionally, while stress deprivation modulated Mmp-3 but not Mmp-13, TR100 increased both Mmp-3 and Mmp-13. The greater response by TR100 treatment of cells could indicate the greater level of F-actin reduction achieved by directly perturbing actin by TR100 treatment as compared with stress deprivation, which may not have as vast an effect on reducing F-actin. We suspect TR100 increases G/F-actin to a greater degree. However, we could not perform a direct comparison of G/F-actin between stress-deprived tendons and cultured tenocytes as biochemical analysis of G/F-actin in matrix-laden tissues is a challenge. A future direction, to determine whether TR100 has a greater effect on reducing F-actin than stress deprivation, is to compare G/F-actin, via our quantitative imaging approach, in mechanically stimulated tendon explants cultured in the presence of TR100 versus the stress-deprived explants. Ideally, this would require loading tendon cells with cyclical stretch, which has been shown to repress tendinosis-like gene changes (Wunderli *et al.*, 2018).

While it remains unclear how the reduction of F-actin regulates gene expression in tendon cells, the regulation of genes by an increase in G/F-actin can occur through cytoplasmic shuttling of transcription factors such as myocardin-related transcription factor (MRTF), Yes-associated protein (YAP), and/or SCX. In chondrocytes and lens cells, we have shown that an increase in G/F-actin can directly regulate gene expression by controlling the cytoplasmic/nuclear shuttling of MRTF (Parreno *et al.*, 2014, 2017, 2018, 2020). The export of MRTF from the nucleus to the cytoplasm, caused by an increase in G/F-actin, has been associated with down-regulation of Col1, Tnc, and αsma expression as well as up-regulation of Sox9 (Parreno *et al.*, 2014, 2017, 2020). There are limited data that show the regulation of Scx, Mmp-3, and Mmp-13 by MRTF. However, MRTF has been shown to regulate another Mmp, Mmp-12, in nucleus pulposus cells (Song *et al.*, 2022). In support of the potential gene regulation by MRTF in tendon cells, we determined that TR100 reduces nuclear MRTF (Supplemental Figure S1). In addition to MRTF, the presence of F-actin stress fibers has also been shown to be associated with nuclear YAP. In support of the gene regulation by YAP, a recent study determined that small interfering RNA knockdown of Yap increases the expression of Mmp-3 and Mmp-13, while overexpression reduces these levels (Jones *et al.*, 2022). YAP may also regulate tenogenic genes, as we found that exposure of tendon cells to a known YAP inhibitor, verteporfin (Wang *et al.*, 2016; Wei *et al.*, 2017; Delve *et al.*, 2020), reduces tenogenic mRNA levels (Supplemental Figure S2). We did not observe regulation of chondrogenic genes by verteporfin treatment. Therefore, the regulation of chondrogenic genes by actin may be via another mechanism. Finally, in the present study, we identified a decrease in the nuclear proportion of transcription factor SCX by TR100 treatment. To our knowledge, this is the first study to associate F-actin depolymerization regulation to SCX localization. SCX is known to regulate Sox9 expression, collagen synthesis, and the myofibroblast phenotype acquisition (Lejard *et al.*, 2007; Espira *et al.*, 2009; Furumatsu *et al.*, 2010; Roche *et al.*, 2016). Therefore, the decreased nuclear SCX may explain the up-regulation of Sox9 by TR100. Additionally, Scx localization may also contribute to the down-regulation of Col1, Tnc, and αsma mRNA levels that we found in the present study. The potential regulation of tenogenic genes by MRTF, YAP, and SCX could support the notion that tenogenic genes are more sensitive to slight increases in G/F-actin, as multiple pathways regulate their expression. In consideration of the current collective pieces of data, it appears as though multiple signaling pathways downstream of actin contribute to gene regulation in tenocytes. Future studies are required to comprehensively delineate the downstream mechanisms of F-actin polymerization as well as their potential interactions to regulate gene expression in a coordinated manner.

Because we demonstrate that F-actin is regulated by Tpm3.1, this could lead to the speculation that Tpm3.1 plays a role in tendinosis. Tendon overload is often regarded as a cause of tendinosis. It has been suggested that tendon overload causes a paradoxical stress deprivation of tendon cells (Lavagnino *et al.*, 2015b). In support of this mechanotransmission paradox, ex vivo overloading of rat tail tendon has been shown to result in cellular–matrix disruptions (Ros *et al.*, 2019). We speculate that cellular–matrix disruption leads to cellular stress deprivation and destabilization of F-actin. We predict Tpm(s) to be involved in F-actin destabilization as Tpms have been shown to be mechanoregulated in tendon cells; Ralphs *et al.* (2002) have shown that in vitro mechanical stimulation of tendon cells elevates protein expression of Tpm (Ralphs *et al.*, 2002). Our prediction that Tpm3.1 contributes to tendinosis are based mostly on our interpretations from mouse tissue and cell data in this study. Examining whether overloading of human tendon explants reduces Tpm3.1 and/or disrupts the interaction between Tpm3.1 and F-actin is required. Furthermore, future studies are needed to delineate the role that Tpm3.1 plays in F-actin destabilization by stress deprivation using an in vivo model of tendinosis.

In conclusion, F-actin is a critical mediator of cellular phenotype and determining the regulation of F-actin networks by Tpms in tissues could lead to new therapeutic interventions that could prevent and/or reverse progression of disease in various tissue types including tendon.

MATERIALS AND METHODS

Request a protocol through *Bio-protocol*.

Mice and tissue isolation

Wild-type mice, 8–10 wk of age, in the C57BL/6J background were used for experiments. Both female and male mice were used in this study, and data shown are aggregate of both sexes; our experiments determined that cells from both females and males responded similarly to a reduction in F-actin (unpublished data not shown). All procedures were conducted following approved animal protocols from the University of Delaware. Following killed, plantaris, Achilles, and tail tendons were isolated as previously described (Lee and Elliott, 2017, 2019; Lee *et al.*, 2017). To dissect plantaris and Achilles tendons, approximately 1 cm of the plantaris and Achilles complex was removed with the calcaneus intact. The tendons were separated by removing excess surrounding soft tissue before cutting off the calcaneal insertion (Lee and Elliott, 2019). Tail tendon fascicles were obtained from excised tails using forceps (Lee *et al.*, 2017).

Tendon explant stress deprivation culture

Tendon stress deprivation was performed by placing isolated tendon fascicles in culture vessels submerged in serum-free DMEM (GenClone; Genesee Scientific, San Diego, CA) consisting of 1% antimycotic/antibiotic (MilliporeSigma, Burlington, MA) (Gardner *et al.*, 2008; Wunderli *et al.*, 2018, 2020; Jafari *et al.*, 2019). Tendons were maintained at 37°C and 5% CO_2 and were harvested at set time points, either 1 or 2 d post isolation. For these studies, tail tendon fascicles were distributed in a nonbiased manner of experimental conditions, with freshly isolated fascicles serving as controls.

Tail tenocyte isolation and Tpm3.1 inhibition by TR100 treatment

To obtain tendon cells, tail tendon fascicles were isolated and immersed in 0.2% collagenase A (MilliporeSigma) and maintained at 37°C. Following overnight incubation, digests were strained through 100 µm filters and then centrifuged at 600 × *g* for 6 min. Tenocyte pellets were resuspended in fresh DMEM consisting of 10% fetal bovine serum (FBS; GenClone) and 1% antimycotic/antibiotic. For experiments, cells were counted and then seeded on culture vessels at a density between 5 and 10 × 10^3 cells/cm^2. Every 2 d, spent media was replaced with fresh media. Once tenocyte cultures reached ~70% confluency, cells were serum starved in DMEM consisting of 0.5% FBS and 0.1% antimycotic/antibiotic with or without Tpm3.1 inhibitor (TR100; 1–10 µM; MilliporeSigma). Tendon cells were harvested 1 or 2 d after drug treatment.

Human cell culture and Tpm3.1 inhibition by TR100 treatment

Human tenocytes used in the study were purchased from Zen-Bio (Durham, NC). The tenocytes were originally isolated, by enzymatic treatment, from the Achilles tendon of a 59-yr-old male. The resulting cells were validated to express tendon markers: Col1, Scleraxis (Scx), type 3 collagen, and thrombospondin-4. Cells were maintained in DMEM consisting of 10% FBS and 1% antimycotic/antibiotic at 37°C and 5% CO_2. Media was replenished every 2–3 d. Cells were cultured until 70–90% confluency, at which point they were detached from culture flasks using 0.25% trypsin-EDTA (GenClone) and seeded onto new flasks. For experiments, tenocytes at passage 6 or 7 were used and seeded at a density of 2.5 × 10^4 cells/cm^2 onto culture vessels. After 2 d, cells were serum starved in DMEM consisting of 0.5% FBS and 0.1% antimycotic/antibiotic with or without 4 µM TR100. Human cells were harvested 1 d after drug treatment.

Light microscopy and cell area/circularity quantification

Following 24 h of treatment, cells were imaged using a microscopy camera (Swiftcam Technologies, Hong Kong) attached to an Axiovert 25 inverted phase-contrast microscope (Zeiss, Jena, Germany). The boundaries of individual cells were manually traced on images using FIJI software. Cell area and circularity were calculated using FIJI software algorithms as previously performed (Parreno *et al.*, 2014). Circularity was defined as $C = 4\pi(A/P^2)$, where P is the perimeter and A is the cell area. A circularity value of 0 indicates an elongated ellipse, whereas a value of 1 indicates a perfect circle.

Cell viability assay

We used a propidium iodide exclusion assay to quantify the proportion of live cells following TR100 treatment. Cells on culture vessels were placed in 0.05% trypsin at 37°C. After 5 min, cells were centrifuged, and pellets were then resuspended in phosphate-buffered saline (PBS) containing 0.5 µg/ml propidium iodide. Propidium iodide is impermeable to live cells but is incorporated into dead cells with compromised cell membranes. A Tali Image-based Cytometer (Thermo Fisher Scientific, Waltham, MA) was used to calculate the portion of cells in suspension that incorporated propidium iodide. Cells exposed to 70% ethanol served as dead controls.

For visualization of cell viability, cells on culture vessels were stained with 1 µM calcein AM (live cell stain) and 1 µM propidium iodide in PBS at 37°C. After 10 min, cells were rinsed with PBS and visualized using a Zeiss Axio Observer 7 microscope. Cells fixed in 4% paraformaldehyde (before staining) were used as dead cell control.

RNA isolation, gene expression, and Tpm sequencing

For RNA processing, tendon tissue or cultured tendon cells were immersed in TRIzol (Sigma-Aldrich, Burlington, MA) and stored frozen until further use. To extract RNA from tissues, tissues were manually ground in TRIzol using a pellet pestle. RNA was separated via phase separation with chloroform, followed by selective recovery of total RNA using an RNA spin column clean-up kit (RNA Clean & Concentrator-5; Zymo, Irvine, CA). RNA was extracted from cultured cells by phase separation with chloroform followed by RNA precipitation in isopropanol as previously described (Parreno *et al.*, 2020). Reverse transcription of RNA to cDNA was performed using the UltraScript 2.0 cDNA Synthesis Kit (PCR Biosystems, Wayne, PA).

Semi-quantitative RT-PCR was performed using PCRBIO Taq Mix Red solution (PCR Biosystems, London, UK) on equivalent amounts of cDNA using previously validated Tpm primers (Cheng *et al.*, 2018). PCR products were run on a 2% agarose gel. Gel bands were excised and melted, and DNA was purified using the GenCatch Advance Gel Extraction Kit (Epoch Life Sciences, Missouri City, TX). Purified DNA was sequenced using Sanger sequencing (Genewiz, South Plainfield, NJ).

Relative real-time RT-PCR was performed using the qPCRBio Sygreen Blue Mix (PCR Biosystems, Wayne, PA) according to the manufacturer's directions. Each reaction contained 20 ng of cDNA in a 10 µl volume using mouse primers and human primers that are listed in Tables 1 and 2, respectively. Real-time PCR was conducted on a Cielo 3 PCR machine (Azure, Houston, TX).

WES capillary electrophoresis

Total protein was extracted as previously described (Parreno *et al.*, 2020) with slight modifications. Briefly, protein was extracted in 1× radioimmunoprecipitation (RIPA) lysis buffer (MilliporeSigma) and then quantified using a bicinchoninic acid (BCA) protein assay (Prometheus Protein Biology Products; Genesee Scientific). Specific protein levels were determined using a WES Capillary-Based Electrophoresis assay with a 12–230 kDa separation module kit following the manufacturer instructions (Protein Simple, San Jose, CA) with equal volumes of control and experimental protein. The antibodies used for experiments are rabbit anti–pan-actin (1:100; #4968; Cell Signaling), mouse anti-αSMA (1:50; ab7817; Abcam), and rabbit anti-MMP-3 (1:10; EP1186Y; Abcam). Secondary antibodies used were anti-rabbit or anti-mouse HRP-conjugate (Protein Simple). Specific protein levels were normalized to total protein. Total protein values were determined using a Chemiluminescent WES Simple Western Size-Based Total Protein Assay (Protein Simple).

Immunostaining of native tendon

Whole tendons were placed in 4% paraformaldehyde in PBS (GenClone) at 4°C for 2 h. Fixed tendons were then washed three times in PBS and incubated in permeabilization/blocking buffer (PBS containing 0.3% Triton, 0.3% bovine serum albumin, and

Gene	Forward primer	Reverse primer	Product size (base pairs)	Accession no.
18S	GCAATTATTCCCCATGAACG	GGCCTCACTAAACCATCCAA	123	NR_003278.3
Gapdh	TTCGAGAGTCAGCCGCATTT	ATCCGTTGACTCCGACCTTC	79	NM_001289726.1
αsma	TCACCATTGGAAACGAAC	CCCCTGACAGGACGTTGTTA	162	NM_007392.3
Acan	GAAAACTTCGGGGTGGG	TCCCTCTGTGACATTACGGG	96	NM_007424.3
Col1	AGCACGTCTGGTTTGGAGAG	GACATTAGGCGCAGGAAGGT	112	NM_007742.4
Mmp-3	GGTGACCCCACTCACTTTCT	GGCATGAGCCAAGACTGTTC	124	NM_010809.2
Mmp-13	AGACCCCAACCCTAAGCATC	ATAGGGCTGGGTCACACTTC	53	NM_008607.2
Scx	CCACTGAAGAGTCACGGAGA	CTGTTCATAGGCCCTGCTCA	111	NM_198885.3
Sox9	AGTACCCGCATCTGCACAAC	TACTTGTAATCGGGGTGGTCTT	145	NM_011448.4
Tnc	TGGAATTGCTCCCAGCATCC	CCGGTTCAGCTTCTGTGGTAG	65	NM_011607.3

TABLE 1: Real-time RT-PCR mouse primers.

3% goat serum) at room temperature. After 2 h, tendons were transferred into a primary antibody solution containing 1:100 mouse anti-Tpm3.1 antibody (2G10.2; MilliporeSigma) in permeabilization/blocking solution. After overnight incubation at 4°C, tendons were washed six times in PBS and placed in secondary antibody solution containing fluorescent CF488 anti-mouse secondary antibody (1:200; Biotium, Fremont, CA), Hoecsht 33342 (1:500; Biotium), and rhodamine-phalloidin (1:20; Biotium) in permeabilization/blocking buffer at room temperature for 2 h in the dark. Tissues were then washed six times in PBS, placed on a glass slide, and mounted using ProLong gold anti-fade reagent (Thermo Fisher Scientific).

To stain for G/F-actin, fixed tendons were placed in permeabilization/blocking buffer at room temperature. After 2 h, tendons were transferred into permeabilization/blocking buffer containing Hoecsht 33342 (1:500), Alexa Fluor DNase-I (1:500; Thermo Fisher Scientific) and rhodamine-phalloidin (1:20).

Immunostaining of cultured cells

Tendon cells cultured on glass-bottomed dishes (World Precision Instruments, Sarasota, FL) were fixed with 4% paraformaldehyde in PBS at room temperature. After 10 min, fixed cells were washed in PBS and kept at 4°C. Tendon cells were immunostained by first being incubated in permeabilization/blocking buffer at room temperature for 30 min. Next, cells were incubated with mouse anti-Tpm3.1 antibody (1:200; 2G10.2; MilliporeSigma), rabbit anti-SCX antibody (1:100; ab58655; Abcam), or rabbit anti-MRTF antibody (1:100; ab49311), diluted into permeabilization/blocking solution. After overnight incubation at 4°C, cells were washed six times in PBS and placed in secondary antibody solution containing CF488 anti-mouse secondary antibody (1:200), Hoechst 33342 (1:500) to stain nuclei, and rhodamine-phalloidin (1:50) to stain F-actin, in permeabilization/blocking buffer at room temperature for 1 h in the dark. Cells were then washed six times in PBS and mounted using ProLong gold anti-fade reagent (Thermo Fisher Scientific).

Confocal fluorescence microscopy

Stained tissues and cells were imaged using a Zeiss LSM880 laser-scanning confocal fluorescence microscope (Zeiss) using a 20× 0.8NA objective or a 63× 1.4NA oil objective. Z-stack images were acquired using 0.5 µm (20× objective) or 0.3 µm (63× objective) step size. Images were processed using Zen software from Zeiss.

G/F-actin in whole-mount confocal images was quantified using FIJI software. Briefly, single optical slice images from the midregion of full z-stack tendon images were analyzed. A rectangular region of interest (ROI) was selected at the center of the images, and channels (red/green/blue) were then separated. The fluorescence intensities within the ROI for each channel were measured. The fluorescence intensities in the green (DNase-I) channels were divided by the fluorescence intensities in the red (phalloidin) channels to obtain DNase-I/phalloidin (G/F-actin) ratios. Finally, the G/F-actin ratios obtained from each ROI were normalized to the average G/F-actin control values (control averages were set to 1). Of note, tendons from control and stress-deprived groups were stained using identical conditions simultaneously, images were acquired using the same settings on the same day, and ROIs were equivalent in size.

Statistical analysis

Each experiment was replicated at least three times on separate occasions. Data from individual experiments are expressed as a percentage of the control average, which was set to 100. Graphpad Prism 9 (San Diego, CA) was used for statistical analysis. Outliers in pooled data points were identified using the ROUT method with a maximum desired false discovery rate (Q) set at 1% (Motulsky and Brown, 2006). Differences between two groups of data were detected using unpaired *t* tests. Differences between several experimental groups against a control were detected using analysis of variance followed by Dunnett post hoc tests.

Gene	Forward primer	Reverse primer	Product size (base pairs)	Accession no.
18S	GTAACCCGTTGAACCCCATT	CCATCCAATCGGTAGTAGCG	151	K03432.1
Col1	CGGCTCCTGCTCCTCTTAG	CACACGTCTCGGTCATGGTA	137	NM_000088.3
Mmp-13	TGAGTTCGGCCACTCCTTAG	AAACATGAGTGCTCCAGGGT	58	NM_002427.4
Scx	GAACTTTCTGCGCTGGCTTT	CACAAGATGCCATCACACAGT	51	NM_001080514.3

TABLE 2: Real-time RT-PCR human primers.

ACKNOWLEDGMENTS

We thank Thomas Manzoni, Grace Emin, and Sofia Gonzalez-Nolde for critical reading of the manuscript. We also thank Sofia Gonzalez-Nolde for technical expertise in designing and validating the real-time RT-PCR primers used in this study. K.L.I. and K.M.M.E. were supported by the University of Delaware Summer Scholars Program. K.L.I. was supported by the Delaware INBRE Winter Scholars Program. The research reported in this project was supported by a University of Delaware Research Fund—Strategic Initiatives (UDRF-SI) grant, the Delaware Center for Musculoskeletal Research from the National Institutes of Health's National Institute of General Medical Sciences under grant number P20GM139760, and the National Institute of Arthritis and Musculoskeletal and Skin Diseases under grant number R01AR080059.

REFERENCES

Arnoczky SP, Lavagnino M, Egerbacher M (2007a). The mechanobiological aetiopathogenesis of tendinopathy: is it the over-stimulation or the under-stimulation of tendon cells? Int J Exp Pathol 88, 217–226.

Arnoczky SP, Lavagnino M, Egerbacher M, Caballero O, Gardner K (2007b). Matrix metalloproteinase inhibitors prevent a decrease in the mechanical properties of stress-deprived tendons: an in vitro experimental study. Am J Sports Med 35, 763–769.

Arnoczky SP, Lavagnino M, Egerbacher M, Caballero O, Gardner K, Shender MA (2008). Loss of homeostatic strain alters mechanostat "set point" of tendon cells in vitro. Clin Orthop Relat Res 466, 1583–1591.

Arnoczky SP, Tian T, Lavagnino M, Gardner K (2004). Ex vivo static tensile loading inhibits MMP-1 expression in rat tail tendon cells through a cytoskeletally based mechanotransduction mechanism. J Orthop Res 22, 328–333.

Bagchi RA, Czubryt MP (2012). Synergistic roles of scleraxis and Smads in the regulation of collagen 1alpha2 gene expression. Biochim Biophys Acta 1823, 1936–1944.

Bell R, Gendron NR, Anderson M, Flatow EL, Andarawis-Puri N (2018). A potential new role for myofibroblasts in remodeling of sub-rupture fatigue tendon injuries by exercise. Sci Rep 8, 8933.

Blangy A, Bompard G, Guerit D, Marie P, Maurin J, Morel A, Vives V (2020). The osteoclast cytoskeleton—current understanding and therapeutic perspectives for osteoporosis. J Cell Sci 133, jcs244798.

Bonello TT, Janco M, Hook J, Byun A, Appaduray M, Dedova I, Hitchcock-DeGregori S, Hardeman EC, Stehn JR, Bocking T, Gunning PW (2016). A small molecule inhibitor of tropomyosin dissociates actin binding from tropomyosin-directed regulation of actin dynamics. Sci Rep 6, 19816.

Bryce NS, Schevzov G, Ferguson V, Percival JM, Lin JJ, Matsumura F, Bamburg JR, Jeffrey PL, Hardeman EC, Gunning P, Weinberger RP (2003). Specification of actin filament function and molecular composition by tropomyosin isoforms. Mol Biol Cell 14, 1002–1016.

Chatterjee M, Muljadi PM, Andarawis-Puri N (2022). The role of the tendon ECM in mechanotransduction: disruption and repair following overuse. Connect Tissue Res 63, 28–42.

Chen W, Deng Y, Zhang J, Tang K (2015). Uniaxial repetitive mechanical overloading induces influx of extracellular calcium and cytoskeleton disruption in human tenocytes. Cell Tissue Res 359, 577–587.

Cheng C, Nowak RB, Amadeo MB, Biswas SK, Lo WK, Fowler VM (2018). Tropomyosin 3.5 protects the F-actin networks required for tissue biomechanical properties. J Cell Sci 131, jcs222042.

Delve E, Co V, Regmi SC, Parreno J, Schmidt TA, Kandel RA (2020). YAP/TAZ regulates the expression of proteoglycan 4 and tenascin C in superficial-zone chondrocytes. Eur Cell Mater 39, 48–64.

Egerbacher M, Gardner K, Caballero O, Hlavaty J, Schlosser S, Arnoczky SP, Lavagnino M (2022). Stress-deprivation induces an up-regulation of versican and connexin-43 mRNA and protein synthesis and increased ADAMTS-1 production in tendon cells in situ. Connect Tissue Res 63, 43–52.

Espira L, Lamoureux L, Jones SC, Gerard RD, Dixon IM, Czubryt MP (2009). The basic helix-loop-helix transcription factor scleraxis regulates fibroblast collagen synthesis. J Mol Cell Cardiol 47, 188–195.

Fleischhacker V, Klatte-Schulz F, Minkwitz S, Schmock A, Rummler M, Seliger A, Willie BM, Wildemann B (2020). In vivo and in vitro mechanical loading of mouse Achilles tendons and tenocytes—a pilot study. Int J Mol Sci 21, 1313.

Furumatsu T, Shukunami C, Amemiya-Kudo M, Shimano H, Ozaki T (2010). Scleraxis and E47 cooperatively regulate the Sox9-dependent transcription. Int J Biochem Cell Biol 42, 148–156.

Garbe AI, Roscher A, Schuler C, Lutter AH, Glosmann M, Bernhardt R, Chopin M, Hempel U, Hofbauer LC, Rammelt S, *et al.* (2012). Regulation of bone mass and osteoclast function depend on the F-actin modulator SWAP-70. J Bone Miner Res 27, 2085–2096.

Gardiner MD, Vincent TL, Driscoll C, Burleigh A, Bou-Gharios G, Saklatvala J, Nagase H, Chanalaris A (2015). Transcriptional analysis of micro-dissected articular cartilage in post-traumatic murine osteoarthritis. Osteoarthr Cartil 23, 616–628.

Gardner K, Arnoczky SP, Caballero O, Lavagnino M (2008). The effect of stress-deprivation and cyclic loading on the TIMP/MMP ratio in tendon cells: an in vitro experimental study. Disabil Rehabil 30, 1523–1529.

Gateva G, Kremneva E, Reindl T, Kotila T, Kogan K, Gressin L, Gunning PW, Manstein DJ, Michelot A, Lappalainen P (2017). Tropomyosin isoforms specify functionally distinct actin filament populations in vitro. Curr Biol 27, 705–713.

Gunning PW, Hardeman EC, Lappalainen P, Mulvihill DP (2015). Tropomyosin—master regulator of actin filament function in the cytoskeleton. J Cell Sci 128, 2965–2974.

Hatakeyama J, Nomura M, Wakimoto Y, Inoue S, Li C, Takamura D, Akisue T, Moriyama H (2021). Effects of cyclic tensile strain and microgravity on the distribution of actin fiber and Fat1 cadherin in murine articular chondrocytes. J Biomech 129, 110774.

Huisman E, Lu A, McCormack RG, Scott A (2014). Enhanced collagen type I synthesis by human tenocytes subjected to periodic in vitro mechanical stimulation. BMC Musculoskelet Disord 15, 386.

Jafari L, Savard M, Gobeil F, Langelier E (2019). Characterization of moderate tendinopathy in ex vivo stress-deprived rat tail tendons. Biomed Eng Online 18, 54.

Janco M, Rynkiewicz MJ, Li L, Hook J, Eiffe E, Ghosh A, Bocking T, Lehman WJ, Hardeman EC, Gunning PW (2019). Molecular integration of the anti-tropomyosin compound ATM-3507 into the coiled coil overlap region of the cancer-associated Tpm3.1. Sci Rep 9, 11262.

Jarvinen TA, Jozsa L, Kannus P, Jarvinen TL, Hurme T, Kvist M, Pelto-Huikko M, Kalimo H, Jarvinen M (2003). Mechanical loading regulates the expression of tenascin-C in the myotendinous junction and tendon but does not induce de novo synthesis in the skeletal muscle. J Cell Sci 116, 857–866.

Jones DL, Daniels RN, Jiang X, Locke RC, Evans MK, Bonnevie ED, Srikumar A, Nijsure MP, Boerckel JD, Mauck RL, Dyment NA (2022). Mechano-epigenetic regulation of extracellular matrix homeostasis via Yap and Taz. bioRxiv, 499650.

Kee AJ, Chagan J, Chan JY, Bryce NS, Lucas CA, Zeng J, Hook J, Treutlein H, Laybutt DR, Stehn JR, *et al.* (2018). On-target action of anti-tropomyosin drugs regulates glucose metabolism. Sci Rep 8, 4604.

Khan KM, Cook JL, Bonar F, Harcourt P, Astrom M (1999). Histopathology of common tendinopathies. Update and implications for clinical management. Sports Med 27, 393–408.

Kjaer M, Langberg H, Heinemeier K, Bayer ML, Hansen M, Holm L, Doessing S, Kongsgaard M, Krogsgaard MR, Magnusson SP (2009). From mechanical loading to collagen synthesis, structural changes and function in human tendon. Scand J Med Sci Sports 19, 500–510.

Lavagnino M, Arnoczky SP (2005). In vitro alterations in cytoskeletal tensional homeostasis control gene expression in tendon cells. J Orthop Res 23, 1211–1218.

Lavagnino M, Arnoczky SP, Egerbacher M, Gardner KL, Burns ME (2006). Isolated fibrillar damage in tendons stimulates local collagenase mRNA expression and protein synthesis. J Biomech 39, 2355–2362.

Lavagnino M, Arnoczky SP, Kepich E, Caballero O, Haut RC (2008). A finite element model predicts the mechanotransduction response of tendon cells to cyclic tensile loading. Biomech Model Mechanobiol 7, 405–416.

Lavagnino M, Gardner KL, Arnoczky SP (2015a). High magnitude, in vitro, biaxial, cyclic tensile strain induces actin depolymerization in tendon cells. Muscles Ligaments Tendons J 5, 124–128.

Lavagnino M, Wall ME, Little D, Banes AJ, Guilak F, Arnoczky SP (2015b). Tendon mechanobiology: current knowledge and future research opportunities. J Orthop Res 33, 813–822.

Lee AH, Elliott DM (2017). Freezing does not alter multiscale tendon mechanics and damage mechanisms in tension. Ann NY Acad Sci 1409, 85–94.

Lee AH, Elliott DM (2019). Comparative multi-scale hierarchical structure of the tail, plantaris, and Achilles tendons in the rat. J Anat 234, 252–262.

Lee AH, Szczesny SE, Santare MH, Elliott DM (2017). Investigating mechanisms of tendon damage by measuring multi-scale recovery following tensile loading. Acta Biomater 57, 363–372.

Lee W, Nims RJ, Savadipour A, Zhang Q, Leddy HA, Liu F, McNulty AL, Chen Y, Guilak F, Liedtke WB (2021). Inflammatory signaling sensitizes Piezo1 mechanotransduction in articular chondrocytes as a pathogenic feed-forward mechanism in osteoarthritis. Proc Natl Acad Sci USA 118, e2001611118.
Lejard V, Brideau G, Blais F, Salingcarnboriboon R, Wagner G, Roehrl MH, Noda M, Duprez D, Houillier P, Rossert J (2007). Scleraxis and NFATc regulate the expression of the pro-alpha1(I) collagen gene in tendon fibroblasts. J Biol Chem 282, 17665–17675.
Li C, Luo J, Xu X, Zhou Z, Ying S, Liao X, Wu K (2020a). Single cell sequencing revealed the underlying pathogenesis of the development of osteoarthritis. Gene 757, 144939.
Li X, Wang L, Huang B, Gu Y, Luo Y, Zhi X, Hu Y, Zhang H, Gu Z, Cui J, *et al.* (2020b). Targeting actin-bundling protein L-plastin as an anabolic therapy for bone loss. Sci Adv 6, eabb7135.
Lo IK, Marchuk LL, Hollinshead R, Hart DA, Frank CB (2004a). Matrix metalloproteinase and tissue inhibitor of matrix metalloproteinase mRNA levels are specifically altered in torn rotator cuff tendons. Am J Sports Med 32, 1223–1229.
Lo IK, Marchuk LL, Leatherbarrow KE, Frank CB, Hart DA (2004b). Collagen fibrillogenesis and mRNA levels in the maturing rabbit medial collateral ligament and patellar tendon. Connect Tissue Res 45, 11–22.
Meiring JCM, Bryce NS, Lastra Cagigas M, Benda A, Whan RM, Ariotti N, Parton RG, Stear JH, Hardeman EC, Gunning PW (2019). Colocation of Tpm3.1 and myosin IIa heads defines a discrete subdomain in stress fibres. J Cell Sci 132, jcs228916.
Motulsky HJ, Brown RE (2006). Detecting outliers when fitting data with nonlinear regressiona new method based on robust nonlinear regression and the false discovery rate. BMC Bioinformatics 7, 123.
Mubyana K, Corr DT (2018). Cyclic uniaxial tensile strain enhances the mechanical properties of engineered, scaffold-free tendon fibers. Tissue Eng Part A 24, 1808–1817.
Nemoto M, Kizaki K, Yamamoto Y, Oonuma T, Hashizume K (2013). Tenascin-C expression in equine tendon-derived cells during proliferation and migration. J Equine Sci 24, 17–24.
Neugebauer J, Heilig J, Hosseinibarkooie S, Ross BC, Mendoza-Ferreira N, Nolte F, Peters M, Holker I, Hupperich K, Tschanz T, *et al.* (2018). Plastin 3 influences bone homeostasis through regulation of osteoclast activity. Hum Mol Genet 27, 4249–4262.
Parreno J, Amadeo MB, Kwon EH, Fowler VM (2020). Tropomyosin 3.1 association with actin stress fibers is required for lens epithelial to mesenchymal transition. Invest Ophthalmol Vis Sci 61, 2.
Parreno J, Bianchi VJ, Sermer C, Regmi SC, Backstein D, Schmidt TA, Kandel RA (2018). Adherent agarose mold cultures: an in vitro platform for multi-factorial assessment of passaged chondrocyte redifferentiation. J Orthop Res 36, 2392–2405.
Parreno J, Buckley-Herd G, de-Hemptinne I, Hart DA (2008). Osteoblastic MG-63 cell differentiation, contraction, and mRNA expression in stress-relaxed 3D collagen I gels. Mol Cell Biochem 317, 21–32.
Parreno J, Raju S, Niaki MN, Andrejevic K, Jiang A, Delve E, Kandel R (2014). Expression of type I collagen and tenascin C is regulated by actin polymerization through MRTF in dedifferentiated chondrocytes. FEBS Lett 588, 3677–3684.
Parreno J, Raju S, Wu PH, Kandel RA (2017). MRTF-A signaling regulates the acquisition of the contractile phenotype in dedifferentiated chondrocytes. Matrix Biol 62, 3–14.
Pathan-Chhatbar S, Taft MH, Reindl T, Hundt N, Latham SL, Manstein DJ (2018). Three mammalian tropomyosin isoforms have different regulatory effects on nonmuscle myosin-2B and filamentous beta-actin in vitro. J Biol Chem 293, 863–875.
Premdas J, Tang JB, Warner JP, Murray MM, Spector M (2001). The presence of smooth muscle actin in fibroblasts in the torn human rotator cuff. J Orthop Res 19, 221–228.
Raleigh SM, van der Merwe L, Ribbans WJ, Smith RK, Schwellnus MP, Collins M (2009). Variants within the MMP3 gene are associated with Achilles tendinopathy: possible interaction with the COL5A1 gene. Br J Sports Med 43, 514–520.
Ralphs JR, Waggett AD, Benjamin M (2002). Actin stress fibres and cell-cell adhesion molecules in tendons: organisation in vivo and response to mechanical loading of tendon cells in vitro. Matrix Biol 21, 67–74.
Roche PL, Nagalingam RS, Bagchi RA, Aroutiounova N, Belisle BM, Wigle JT, Czubryt MP (2016). Role of scleraxis in mechanical stretch-mediated regulation of cardiac myofibroblast phenotype. Am J Physiol Cell Physiol 311, C297–C307.
Ros SJ, Muljadi PM, Flatow EL, Andarawis-Puri N (2019). Multiscale mechanisms of tendon fatigue damage progression and severity are strain and cycle dependent. J Biomech 85, 148–156.
Sawadkar P, Player D, Bozec L, Mudera V (2020). The mechanobiology of tendon fibroblasts under static and uniaxial cyclic load in a 3D tissue engineered model mimicking native extracellular matrix. J Tissue Eng Regen Med 14, 135–146.
Sbardella D, Tundo GR, Fasciglione GF, Gioia M, Bisicchia S, Gasbarra E, Ippolito E, Tarantino U, Coletta M, Marini S (2014). Role of metalloproteinases in tendon pathophysiology. Mini Rev Med Chem 14, 978–987.
Schevzov G, Whittaker SP, Fath T, Lin JJ, Gunning PW (2011). Tropomyosin isoforms and reagents. Bioarchitecture 1, 135–164.
Sharma P, Maffulli N (2006). Biology of tendon injury: healing, modeling and remodeling. J Musculoskelet Neuronal Interact 6, 181–190.
Song M, Zhang Y, Sun Y, Kong M, Han S, Wang C, Wang Y, Xu D, Tu Q, Zhu K, *et al.* (2022). Inhibition of RhoA/MRTF-A signaling alleviates nucleus pulposus fibrosis induced by mechanical stress overload. Connect Tissue Res 63, 53–68.
Stauber T, Blache U, Snedeker JG (2020). Tendon tissue microdamage and the limits of intrinsic repair. Matrix Biol 85–86, 68–79.
Stehn JR, Haass NK, Bonello T, Desouza M, Kottyan G, Treutlein H, Zeng J, Nascimento PR, Sequeira VB, Butler TL, *et al.* (2013). A novel class of anticancer compounds targets the actin cytoskeleton in tumor cells. Cancer Res 73, 5169–5182.
Thornton GM, Shao X, Chung M, Sciore P, Boorman RS, Hart DA, Lo IK (2010). Changes in mechanical loading lead to tendonspecific alterations in MMP and TIMP expression: influence of stress deprivation and intermittent cyclic hydrostatic compression on rat supraspinatus and Achilles tendons. Br J Sports Med 44, 698–703.
Tojkander S, Gateva G, Schevzov G, Hotulainen P, Naumanen P, Martin C, Gunning PW, Lappalainen P (2011). A molecular pathway for myosin II recruitment to stress fibers. Curr Biol 21, 539–550.
Tsolis KC, Bei ES, Papathanasiou I, Kostopoulou F, Gkretsi V, Kalantzaki K, Malizos K, Zervakis M, Tsezou A, Economou A (2015). Comparative proteomic analysis of hypertrophic chondrocytes in osteoarthritis. Clin Proteomics 12, 12.
Wang C, Zhu X, Feng W, Yu Y, Jeong K, Guo W, Lu Y, Mills GB (2016). Verteporfin inhibits YAP function through up-regulating 14-3-3sigma sequestering YAP in the cytoplasm. Am J Cancer Res 6, 27–37.
Wang T, Lin Z, Ni M, Thien C, Day RE, Gardiner B, Rubenson J, Kirk TB, Smith DW, Wang A, *et al.* (2015). Cyclic mechanical stimulation rescues achilles tendon from degeneration in a bioreactor system. J Orthop Res 33, 1888–1896.
Wei H, Wang F, Wang Y, Li T, Xiu P, Zhong J, Sun X, Li J (2017). Verteporfin suppresses cell survival, angiogenesis and vasculogenic mimicry of pancreatic ductal adenocarcinoma via disrupting the YAP-TEAD complex. Cancer Sci 108, 478–487.
Wunderli SL, Blache U, Beretta Piccoli A, Niederost B, Holenstein CN, Passini FS, Silvan U, Bundgaard L, Auf dem Keller U, Snedeker JG (2020). Tendon response to matrix unloading is determined by the patho-physiological niche. Matrix Biol 89, 11–26.
Wunderli SL, Widmer J, Amrein N, Foolen J, Silvan U, Leupin O, Snedeker JG (2018). Minimal mechanical load and tissue culture conditions preserve native cell phenotype and morphology in tendon—a novel ex vivo mouse explant model. J Orthop Res 36, 1383–1390.
Yuan T, Zhang J, Zhao G, Zhou Y, Zhang CQ, Wang JH (2016). Creating an animal model of tendinopathy by inducing chondrogenic differentiation with kartogenin. PLoS One 11, e0148557.
Zhang J, Wang JH (2013). The effects of mechanical loading on tendons—an in vivo and in vitro model study. PLoS One 8, e71740.
Zhao S, Cai J, Zhang X, Cui J, Jiu Y (2020). Different formins restrict localization of distinct tropomyosins on dorsal stress fibers in osteosarcoma cells. Cytoskeleton 77, 16–24.